



---

## Effect of *Spondias mombin* Extract on the Corrosion of Mild Steel in Acid Media

Godwin Abawulo Ijuo\*, Apeh Michael Orokpo, Priscilla Ngunoon Tor

Chemistry Department, University of Agriculture, Makurdi, Nigeria

**Abstract** The influence of *Spondias mombin* (SM) extract on the corrosion behavior of mild steel (MS) in 1.0 M HCl was studied using weight loss and electrochemical polarization techniques. The results revealed that SM was an excellent green inhibitor and the inhibition efficiency (%IE) obtained from weight loss and electrochemical experiments were in good agreement. Electrochemical polarization data revealed the mixed mode of inhibition of SM. Thermodynamic studies revealed that corrosion inhibition may be due to the spontaneous physical adsorption of the plant constituents on the surface of mild steel. Kinetic study of the plants followed a pseudo first order reaction. FTIR spectra and optical micrographs confirmed the adsorption of SM on the mild steel surface. The adsorption of inhibitors on mild steel surface obeys the Langmuir and Freundlich adsorption isotherm models. Synergism parameter evaluated was found to be greater than unity for all concentrations of inhibitor indicating that the increase in the inhibition efficiency of SM was due to the presence of iodide (I<sup>-</sup>) ions.

**Keywords** Corrosion inhibitor, *Spondias mombin*, mild steel, Adsorption isotherm

---

### Introduction

Corrosion is a known major destructive process affecting the performance of metallic materials in applications in many construction sectors. It is a naturally occurring phenomenon defined as deterioration of metals and their alloys caused by their action with the surrounding environmental conditions.

Just like other natural hazards such as earthquakes or severe weather disturbances, corrosion can cause dangerous and expensive damage to everything from vehicles, home appliances, and water and waste-water systems to pipelines, bridges, and public buildings. Unlike weather-related disasters, however, there are time-proven methods to prevent and control corrosion that can reduce or eliminate its impact on public safety, the economy, and the environment. The science of corrosion prevention and control is highly complex, exacerbated by the fact that corrosion takes many different forms and is affected by numerous external factors as reported by Tao *et al* [1]. To prevent or minimize internal corrosion in these systems, inhibitors are used especially in flow and closed systems, such as fresh water distribution systems.

A Corrosion inhibitor is a substance which when added in small concentration to an environment, effectively reduces the corrosion rate of a metal exposed to it. Large numbers of organic compounds have been studied and are still being studied to assess their corrosion inhibition potential.

However, most of these substances are not only expensive but also pose health and environmental hazards [2] causing the search for their replacement. Recently, a lot of research efforts have gone into the search for non-toxic naturally occurring substances for use as metal/alloy corrosion inhibitors. The exploration of natural products of plant origin as inexpensive and eco-friendly corrosion inhibitors is an essential field of study. In addition to being environmental friendly and ecologically acceptable, plant products are low-cost, readily available and renewable



sources of materials. On this basis, a number of amino acids [3] as well as extracts from leaves, roots and stem barks of plant (biomass) and even fruits or fruit peels have been reported as effective inhibitors of metal and alloy corrosion in different aggressive environments [4].

*Spondias mombin* (Mombins) is a species of flowering plant in the family Anacardiaceae. It is native to the tropical Americas, including the West Indies. The tree has been naturalized in parts of Africa, India, Bangladesh, Sri Lanka and Indonesia. Phytochemical screening of the plant revealed that the leaves contain saponins, alkaloids and tannins while flavonoids, alkaloids and tannins were detected in all the extraction media of the stem bark. The leaf extract contained more vitamin C and E than the stem bark extracts [5]. The present study investigates the inhibitory action of *Spondias mombin* extracts on the corrosion of mild steel in HCl with a view to establishing its potential as a corrosion inhibitor of mild steel in acidic medium and understanding its mechanism of adsorption on the mild steel surface.

## Experimental Work

### Materials

The mild steel coupons used in the experiment were press cut as rectangular coupons of dimensions of 2 cm x 3 cm x 0.14 cm. Before each experiment, the mild steel coupons were wet polished with emery paper, rinsed with distilled water, dried in acetone and warm air, weighed and stored in a moisture-free desiccator. The acid solution (1.0M HCl) gotten from Emole chemicals in Makurdi was prepared by diluting analytical (AR grade 98%) HCl in distilled water.

Fourier Transform Infrared Spectroscopy (FTIR) was carried out using FTIR-8400S FOURIER TRANSFORM INFRARED SPECTROPHOTOMETER instrument.

TSVIEW DIGITAL METALLURGICAL MICROSCOPE, MODEL: TUCSEN 0923502 was employed to observe the surface morphologies of the metals.

### Inhibitor Preparation

Air-dried stem bark of *SM* (504g) were pulverized into fine powder and extracted exhaustively with methanol at room temperature. Concentration of the combined methanol extract yielded a dark green extract of methanol (126 g). This was used for the corrosion inhibition studies. The inhibitor was dissolved in 1.0 M HCl at different concentrations ranging from 0.2g/L to 1.0g/L. The 1.0 M HCl in the absence of inhibitor was taken as blank for comparison.

### Weight loss measurement

The effect of immersion time and temperature was carried out using weight loss measurement. The effect of temperature was carried out at 303, 313, 323 and 333 K using the method of [06]. Weight loss measurement was conducted on the pre-cleaned and weighed coupons suspended in beakers (maintained at 303, 313, 323 and 333K respectively) containing the test solutions using glass hooks and rods. Tests were conducted under total immersion conditions in 200 mL of the aerated and unstirred test solutions. The coupons were weighed after 3 hours of immersion in the test solution. To determine weight loss with respect to time, the coupons were immersed in 20% NaOH solution containing 200 g/L of zinc dust, scrubbed with bristle brush, washed, dried and weighed then immersed in beakers containing 200 mL test solutions using glass hooks and rods and retrieved at 24-h intervals for 168 h. The weight loss was taken to be the difference between the weight of the coupons at a given time and its initial weight. The experiment was run in duplicates to obtain good reproducible data. Average values for each experiment was obtained and used in subsequent calculations.

$$IE_{\text{exp}} = \left(1 - \frac{W_{(1)}}{W_{(0)}}\right) \times 100 \quad (01)$$

Where  $W_{(0)}$  is the weight loss of the mild steel without inhibitor and  $W_{(1)}$  is the weight loss of mild steel with inhibitor.



### Electrochemical measurement

The coupon was sealed with epoxy resin in such a way that only one square surface area was left uncovered. The exposed surface was degreased in acetone, rinsed with distilled water and dried in warm air. Electrochemical experiment was conducted in a conventional three-electrode cell voltammeter. Mild steel specimen was used as a working electrode, platinum (Pt) electrode and saturated calomel electrode (SCE) served as auxiliary and reference electrodes, respectively. All electrochemical experiments was conducted at room temperature ( $27\pm 2$  °C) using 100 mL of test solution. Before the potentiodynamic polarization (Tafel), the electrode was allowed to corrode freely and its open circuit potential (OCP) was recorded as a function of time up to 30 min. AC impedance measurements was carried out at the corrosion potential ( $E_{\text{corr}}$ ) with frequency range from 100,000 to 0.1 Hz at an amplitude of 10 mV and scan rate of 10 points per decade. The %IE was calculated from the charge transfer resistance ( $R_{\text{ct}}$ ) values by using the equation

$$\%IE = \frac{R_{\text{ct}(1)} - R_{\text{ct}(0)}}{R_{\text{ct}(1)}} \times 100 \quad (02)$$

Where,  $R_{\text{ct}(0)}$  is the charge transfer resistance of MS without inhibitor and  $R_{\text{ct}(1)}$  is the charge transfer resistance of MS with inhibitor. The Tafel polarization curves will be recorded by scanning the electrode potential from -300 mV to 300 mV (*vs* SCE) with a scanning rate of 1 mV/s. The linear Tafel segments of the anodic and cathodic curves was extrapolated to corrosion potential to obtain the corrosion current densities ( $I_{\text{corr}}$ ). The %IE was obtained from the equation below

$$\%IE = \frac{I_{\text{corr}(0)} - I_{\text{corr}(1)}}{I_{\text{corr}(0)}} \times 100 \quad (03)$$

Where,  $I_{\text{corr}(0)}$  is the corrosion current densities of MS without inhibitor and  $I_{\text{corr}(1)}$  is the corrosion current densities of MS with inhibitor.

### Fourier transform infrared spectroscopy

The inhibitor was characterized by Fourier Transform Infrared Spectrophotometer (FTIR) for identification of active functional groups.

### Optical microscopy

Optical microscopy was employed to observe the surface morphologies of the metals. For this study, finely polished MS coupons were immersed in 1.0 M HCl solution in the presence and absence of 0.2g/L of inhibitor for 24hrs. Then the specimens were cleaned with distilled water and acetone, dried and used for the analysis.

## Results and Discussion

### Gravimetric data

#### Effect of time on the corrosion rate of mild steel in 1.0 M HCl in the presence and absence of SM

The effect of time on the corrosion rate of mild steel in free acid and in the presence of different concentrations of the inhibitor was studied in the range of 24-168hrs as shown in figure 3, it was observed that the rate of corrosion increases with increase in time but decreased with increase in concentration



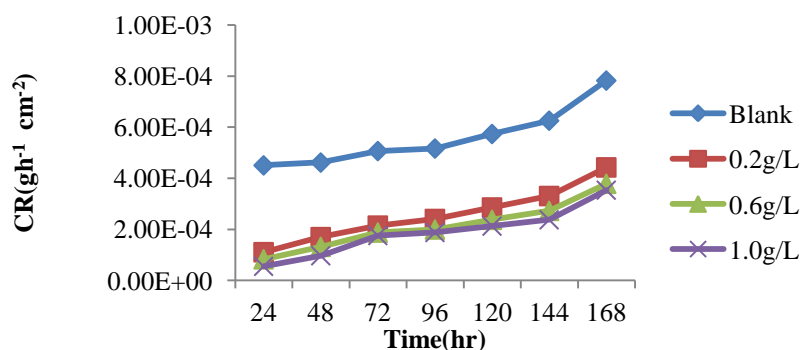


Figure 1: Effect of time on the corrosion rate of mild steel in 1.0 M HCl in the Presence and Absence of SM

### Effect of time on the inhibition efficiency of mild steel in 1.0 M HCl in the presence and absence of SM

The inhibition efficiency of mild steel exposed to different concentrations of the inhibitor at a time range of 24hrs-168hrs is shown in figure 2. The percentage inhibition efficiency of the extracts was found to increase with increasing concentration of acid extracts of the inhibitors but decreased in days as a result of increase in the fraction of the mild steel surface covered by the adsorbed constituents of the extract as the concentration of the plant extracts increases. The highest percentage inhibition efficiency for SM (88.23%) for was recorded at the highest concentration studied at 24hrs.

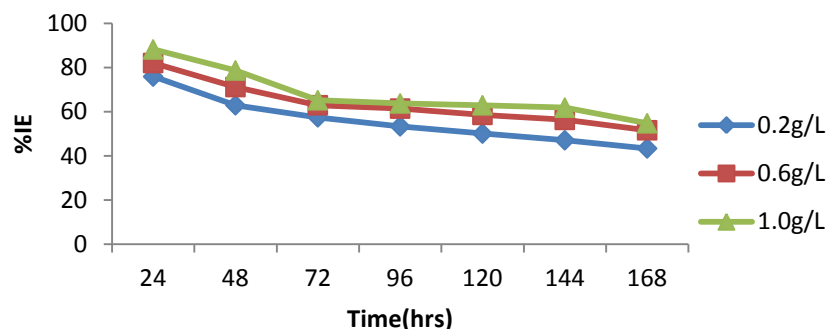


Figure 2: Effect of time on the inhibition efficiency of mild steel in 1.0 M HCl in the presence and absence of SM

### Effect of temperature on the corrosion rate of mild steel in 1.0 M HCl in the presence and absence of SM

The effect of temperature on the corrosion rate of mild steel in free acid and in the presence of different concentrations of the inhibitor(plant extract) was studied in the range of 303-333 K as shown in tables and figure 3. It was observed that the rate of corrosion of mild steel in the absence and presence of different concentrations of the inhibitor increase with increase in temperature. This is expected because as temperature increases, the rate of corrosion of mild steel also increases as a result of increase in the average kinetic energy of the reacting molecules. Moreover the corrosion rate is much decreased for inhibited acid solution than the uninhibited acid solution.

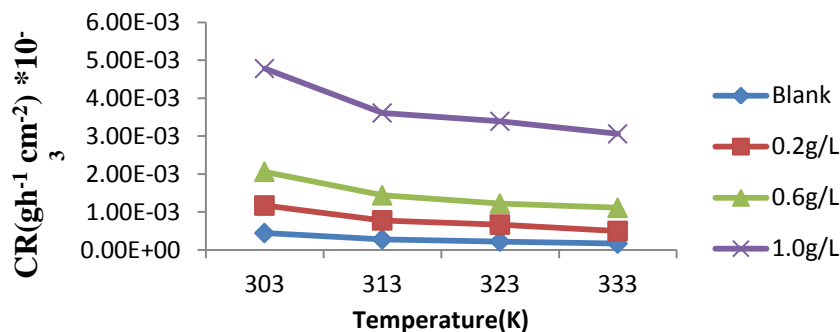


Figure 3: Effect of temperature on the corrosion rate of mild steel in 1.0 M HCl in the presence and absence of SM

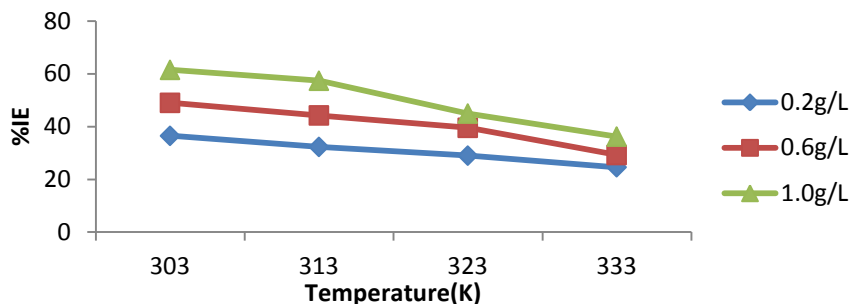


Figure 4: Effect of temperature on the inhibition efficiency of mild steel in 1.0 M HCl in the presence and absence of SM

To evaluate the stability of the adsorbed layer/film of inhibitor on mild steel surface, weight loss measurements were carried out in the range of 303-333 K in the absence and presence of the extract. The results obtained are shown in figure 4. It is evident from these figures that inhibition efficiency decreases with increasing temperature but increased with increase in concentration. This is due to increased rate of dissolution process of mild steel and partial desorption of the inhibitor from the metal surface with temperature [6].

**Table 1:** Gravimetric data for the corrosion of mild steel in 1.0 M HCl in the presence and absence of SM

Concentration	Corrosion rate (CR x 10 <sup>-4</sup> )				Inhibition efficiency (%IE)			
	303K	313K	323K	333K	303K	313K	323K	333K
Blank	0.44	1.17	2.06	4.78	-	-	-	-
0.2 g/L	0.28	0.78	1.44	3.61	36.50	32.30	29.00	24.60
0.6 g/L	0.22	0.67	1.22	3.39	49.00	44.24	39.54	29.23
1.0 g/L	0.17	0.50	1.11	3.06	61.50	57.38	44.95	36.21

### Adsorption consideration

Adsorption isotherms are necessary in determining the mechanism of organo-electrochemical reaction. The inhibition of the corrosion of mild steel in 1.0 M HCl medium with addition of different concentrations of the extract can be explained by the adsorption of the components of the plant extracts on the metal surface. Inhibition efficiency (%) is directly proportional to the surface coverage or fraction of the surface covered by the adsorbed molecule ( $\theta$ ).

$$\theta = \frac{\%IE}{100} \quad (4)$$

Surface coverage data obtained from weight loss experiments were inserted in Temkin, Frumkin, Freundlich and Langmuir adsorption isotherms to verify the nature of interactions between the inhibitors and mild steel surface.

### Langmuir adsorption isotherm

This isotherm is described by the equation (4) as given by Oguzie, [7] and Adeyemi *et al* [8].

$$\frac{C}{\theta} = \frac{1}{K_{ads}} + C \quad (5)$$

where C is the inhibitor concentration,  $K_{ads}$  the Adsorption equilibrium constant and  $\theta$  the surface coverage.

Taking the logarithm of equation (5) above yields equation (6)

$$\text{Log}\left(\frac{C}{\theta}\right) = \text{Log}C - \text{Log}K_{ads} \quad (6)$$

The plot of  $\text{Log}(C/\theta)$  versus C is linear with the intercept equal to  $-\text{Log}K_{ads}$  for the extract (fig.7). The estimated values for  $K_{ads}$ , correlation coefficient ( $r^2$ ), intercept and slope for the extract at various temperatures are shown in the table 4.



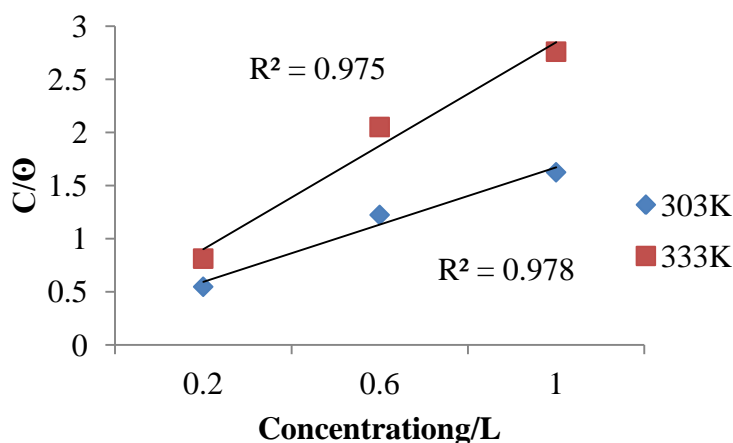


Figure 5: Langmuir adsorption isotherm

### Freundlich adsorption isotherm

A linear plot of  $\log \theta$  against  $\log C$  also shows that the adsorption of inhibitors on mild steel surface in the aqueous medium follows Freundlich isotherm. Hence, the adsorption sites can be assumed to be distributed exponentially with respect to energy of adsorption and that the surface sites are subdivided into several types, each possessing a characteristic heat of adsorption [3]. It can therefore be said that the assumptions of either Langmuir or Freundlich can be used to characterize the nature of adsorption. The linearity shows that the adsorption of the inhibitors on mild steel surface in aqueous medium follows Freundlich isotherm [9].

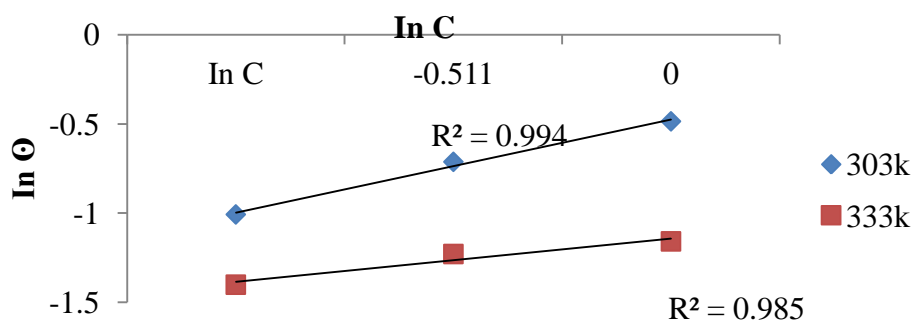


Figure 6: Freundlich adsorption isotherm

### Thermodynamic Study

#### Determination of activation energy

Calculation of the temperature dependence of inhibition as well as comparison of corrosion activation energies in the presence and absence of inhibitor gives some insight into the possible mechanism of inhibitor adsorption. A decrease in temperature in inhibition efficiency, with analogous increase in corrosion activation energy in the presence of inhibitor compared to its absence is always interpreted as being suggestive of formation of an adsorption film of physical (electrostatic) nature. Thus the apparent activation energy ( $E_a$ ), for the corrosion process in the absence and presence of the inhibitor was evaluated from Arrhenius equation [10].

$$\ln \left( \frac{CR_2}{CR_1} \right) = \frac{E_a}{R} \left( \frac{1}{T_1} - \frac{1}{T_2} \right) \quad (7)$$

where  $CR_1$  and  $CR_2$  are the corrosion rate at temperature  $T_1$  and  $T_2$  respectively,  $E_a$  is the apparent activation energy,  $R$  is the molar gas constant.

The estimated values of  $E_a$  for mild steel corrosion in the presence of the plant is listed in the table 1. The data shows that activation energy of the corrosion in mild steel in 1.0 M HCl solution in the presence of *SM* extract is



higher than that in the absence of the inhibitor. Activation energy was found to be 66.12KJ/mol for 1.0 M HCl solution and increases to 76.12KJ/mol.

These shows that the adsorbed organic matter has provided a physical barrier to the change and mass transfer, leading to reduction in corrosion rate as reported by James *et al* [11] and Ebenso *et al* [12]. It has been reported that when the values of  $E_a > 80\text{KJ/mol}$  indicates chemisorption whereas  $E_a < 80\text{KJ/mol}$  infers physisorption [13-14]. On the basis of the experimentally determined activation energy value of  $E_a < 80\text{KJ/mol}$  in this study, we would say that the additive is physically adsorbed on the coupons. Therefore, it is viable that a multilayer protective coverage on the entire mild steel surface was obtained.

**Table 2:** The  $E_a$  values with the various concentrations

System	$E_a$ (KJ/mol)
Blank	66.12
0.2g/L	70.87
0.6g/L	75.81
1.0g/L	80.12

### Determination of enthalpy ( $\Delta H$ ) and entropy ( $\Delta S$ )

Thermodynamic parameters such as enthalpy ( $\Delta H$ ) and entropy ( $\Delta S$ ) of activation of corrosion process may be evaluated from the effect of temperature. They may be calculated with the following equation:

$$\text{Log } CR/T = \text{Log}(R/nh) + \Delta S/2.303R - \Delta H/2.303R \quad (8)$$

Where CR is the corrosion rate at temperature T, R is the molar gas constant, n is Avogadro's constant and h is the Planck's constant. A plot of

$$\text{Log } CR/T \text{ vs } 1/T \quad (9)$$

Is a straight line graph (fig 7) with a slope of

$$(-\Delta H/2.303RT) \quad (10)$$

And an intercept of

$$\text{Log}(R/nh) + \Delta S/2.303R \quad (11)$$

From which the values of  $\Delta H$  and  $\Delta S$  were calculated.

The results presented in tables 3 shows that the enthalpy of activation values are all positive for the extract which shows the endothermic nature of the mild steel dissolution process. Also the entropies of activation energy were positive for the extract, reflecting that the activation complex represents association steps and that the reaction was spontaneous and feasible. These results were in excellent agreement with the reports of previous work by Obot *et al* [15].

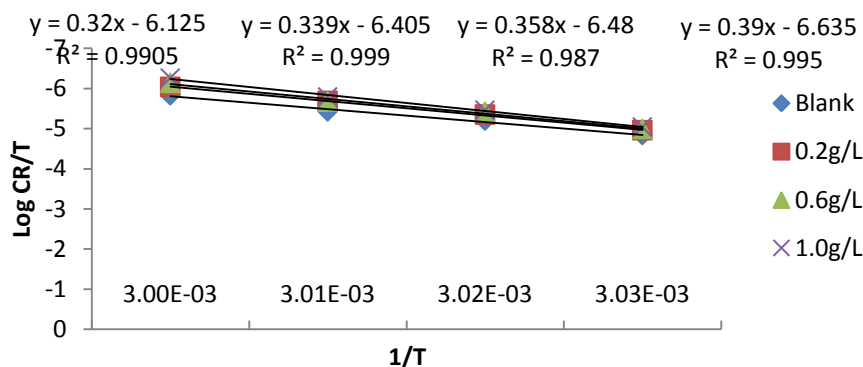


Figure 7: Plot of log CR/T VS 1/T



**Table 3:** Calculated values of enthalpy ( $\Delta H$ ) and entropy ( $\Delta S$ )

System	Enthalpy(KJ/mol)	Entropy(KJ/mol)
Blank	6.13	0.036
0.2g/L	6.49	0.036
0.6g/L	6.85	0.036
1.0g/L	7.47	0.037

### Determination of free energy

The values of  $\Delta G_{ads}$  that can characterize the interaction of adsorption molecules and metal surface was calculated by equation (12) and presented in tables (4 and 5). The negative values of  $\Delta G_{ads}$  describes the spontaneity of adsorption process and stability of the adsorbed layer on the mild steel surface. Whenever, the values of  $\Delta G_{ads}$  is around -20KJ/mol or lower is said to be consistent with physisorption, while those around -40KJ/mol or higher involve chemisorptions as reported by Oguzie *et al* [13]. As shown in table, results obtained indicate that the values of  $\Delta G_{ads}$  are negative in all cases and are less than -20KJ/mol. This agrees with literature survey and authenticates physical adsorption. This means that the plant extracts adheres on the surface of the corroding system and so gives a very strong inhibitor.

$$\Delta G_{ads} = -2.303RT \log (55.5K_{ads}) \quad (12)$$

**Table 4:** Calculated thermodynamic parameters from langmuir adsorption isotherm

Inhibitor	System	Intercept	Slope	$K_{ads}(M^{-1})$	$r^2$	$\Delta G_{ads}(J/mol)$
SM	303K	0.414	1.348	2.415	0.978	-12.34
	333K	0.324	2.436	3.086	0.975	-14.24

**Table 5:** Calculated thermodynamic parameters fomfreundlich adsorption isotherm

Inhibitor	System	Intercept	Slope	$K_{ads}$	$r^2$	$\Delta G_{ads}(KJ/mol)$
SM	303K	-0.513	0.316	3.165	0.994	-13.02
	333K	-1.156	0.152	3.175	0.985	-14.32

### Kinetic study

#### Determination of rate constants and half life

The corrosion reaction is a heterogeneous reaction which is of anodic and cathodic reactions at the same or different rate. It is on this basis that kinetic analysis of the data is considered important. In this present study, the initial weight of mild steel coupon is designated  $W_i$  while the weight after time  $t$ ,  $W_L$  hence the weight change after time  $t$ , ( $W_i - W_L$ ). The rate constant was calculated as shown in previous report James *et al* [11].

$$\ln(W_i - W_L) = -k_1 t + \ln W_L \quad (13)$$

The plots of  $-\log$  weight loss against time (in days) at 303K was studied and shows a linear variation and slope  $k_1$  which confirms a first order reaction kinetics with respect to the corrosion of mild steel in 1.0 M HCl solutions in the presence of the SM





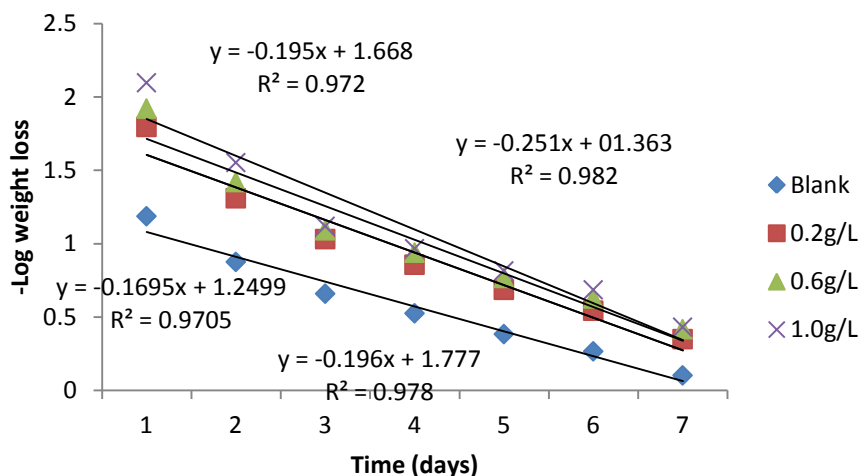


Figure 8: Variation of  $-\text{Log weight loss}$  with time (days) for mild steel coupons in 1.0 M HCl solution containing SM extract

### Half life

The half-life ( $t_{1/2}$ ) was calculated from the relation below as shown in Table 6

$$t_{1/2} = \frac{0.693}{K} \quad (14)$$

The increase in half-life ( $t_{1/2}$ ) shown when the extracts of SM were present further authenticates the inhibition of mild steel in 1.0 M HCl by the additives. As the half-life increases, the corrosion rate decreases which shows that more protection of the metals by the SM extracts has been established. As discussed earlier, the activation energy which is in the range of 66.12 and 73.84 kJ/mol is in an indication that the additive is physically adsorbed on the metal coupons.

**Table 6:** Half-life parameters at various concentrations

System	Rate constant, k, ( $\text{day}^{-1}$ )	Half-life (days)
Blank	0.152	0.218
0.2g/L	0.711	0.975
0.6g/L	0.662	1.046
1.0g/L	0.686	1.009

### Polarization measurement

Linear polarization measurements were undertaken mainly to understand the possible influence of addition of different concentrations of the inhibitors on the anodic dissolution of mild steel and the corresponding cathodic reduction of hydrogen ion of the corrosion process.

The linear polarization curves obtained from the corrosion behavior of MS in 1.0 M HCl in the absence and presence of green inhibitor is shown in figure 9. The electrochemical parameters; corrosion potential ( $E_{\text{corr}}$ ), corrosion current density ( $I_{\text{corr}}$ ), anodic and cathodic Tafel slopes ( $B_a$  and  $B_c$ ) were calculated from the intersection of the anodic and cathodic Tafel lines of the polarization curves at  $E_{\text{corr}}$ . All the parameters obtained from the polarization measurements is listed in Table 6. % IE was calculated by using eq. (15).

From the polarization curves, it can be clearly seen that when compared with blank, both anodic and cathodic curves were shifted toward the direction of lower current density for both inhibitors as the concentration increased. This phenomenon implied that the inhibitors could suppress the anodic reaction of metal dissolution of iron and cathodic hydrogen evolutions with cathodic predominance.

Thus, this reveals that all inhibitors act as mixed-type inhibitor [14, 16].



The corrosion inhibition was calculated from the linear polarization data using the relation in (15):

$$\% IE = \frac{R_{ct(1)} - R_{ct(0)}}{R_{ct(1)}} \times 100 \quad (15)$$

Where,  $R_{ct(0)}$  is the charge transfer resistance of MS without inhibitor and  $R_{ct(1)}$  is the charge transfer resistance of MS with inhibitor. From Table 7, the inhibition of these reactions was more pronounced on the increasing of inhibitor concentration for the inhibitor, reaching value of 94.548% at 1.0g/L. The trend for the inhibition efficiencies were consistent with those obtained from gravimetric analysis. This result agreed with those reported by Vrsalovic *et al* [4].

**Table 7:** Electrochemical polarisation parameters for mild steel in 1.0 M HCl in the presence and absence of *Spondias mombin*

System	$E_{corr}$ (M)	$i_{corr}$ ( $\mu$ a/cm <sup>2</sup> )	$b_a$ (V/dec)	$b_c$ (V/dec)	CR(mm/year)	%IE
Blank	-1577.2	1404.8	-163.33	63.461	16.324	–
0.2g/L	-954.88	256	-78.35	56.93	2.9725	81.779
0.6g/L	-903.89	101	-65.41	43.57	1.1763	92.81
1.0g/L	-872.3	0.766	-55.898	22.626	0.89002	94.548

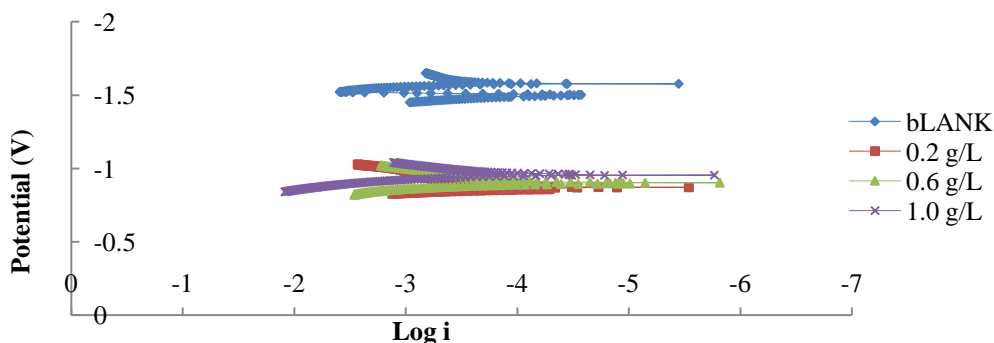


Figure 9: Tafel plot of MS immersed in 1.0 M HCl with and without SM

#### Fourier transform infra-red (FTIR) analysis

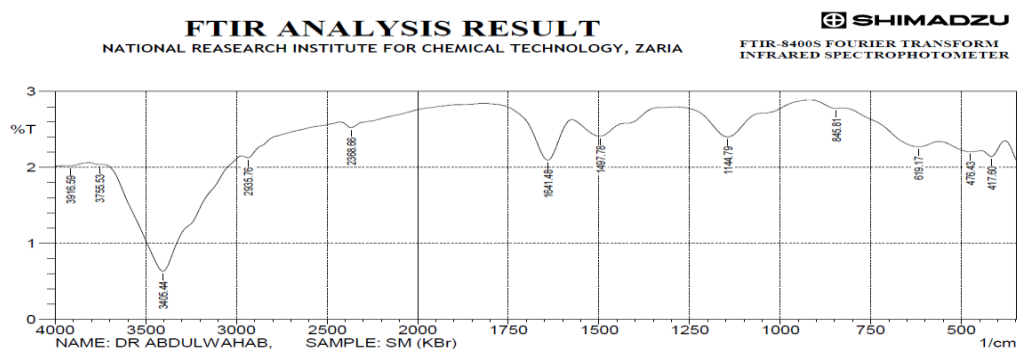


Figure 10: FTIR spectra

The peak at  $3405.44 \text{ cm}^{-1}$  is due to phenolic O-H,  $2935.76 \text{ cm}^{-1}$  correspond to alkyl C-H,  $1641.48 \text{ cm}^{-1}$  is assigned aromatic C=C bending,  $1497.78 \text{ cm}^{-1}$  is assigned aromatic C-H bending the  $845.61 \text{ cm}^{-1}$  is assigned aromatic substitution.

**Table 8:** Important Peaks of Pure and Adsorbed Inhibitors (frequency  $\text{cm}^{-1}$ )

Inhibitor	SM	SM on mild steel
-----------	----	------------------



Phenolic O-H stretch	3405.44	-
Alkyl C-H stretch	2935.76	-
Aromatic C=C bending	1641.48	-
Aromatic C-H bending	1497.78	1825.1
Aromatic substitution	845.66	872.2

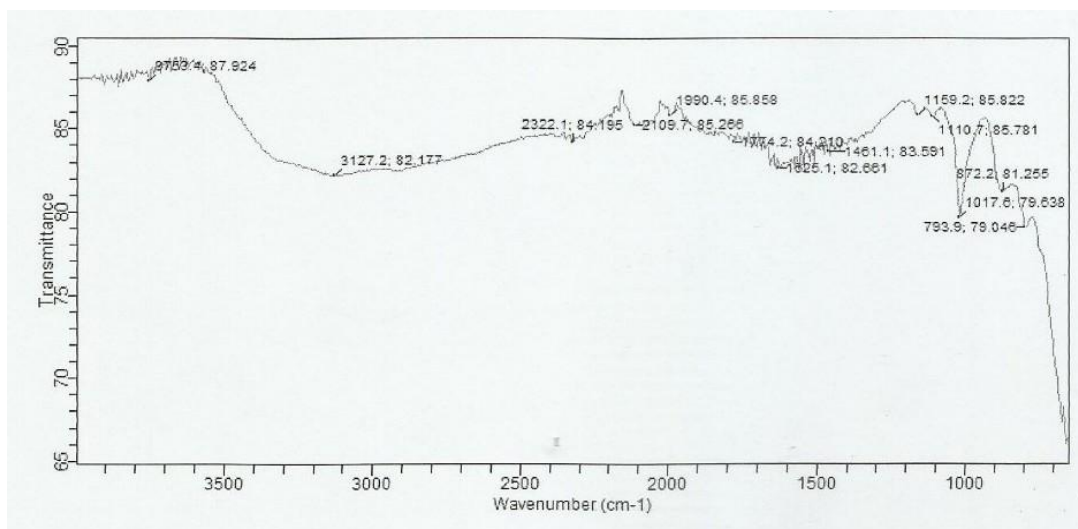
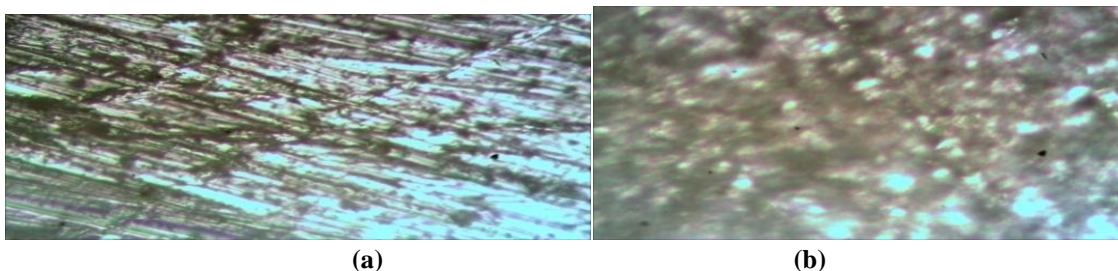


Figure 11: FTIR spectra of SM adsorbed on mild steel in 1.0 M HCl solution

Fig 11 above shows the infrared spectra of SM adsorbed on mild steel in HCl solution. It is evident from the spectra that the peak at  $3405.44\text{ cm}^{-1}$  has disappeared, confirming that oxygen was involved in adsorption, the peak at  $2935.76\text{ cm}^{-1}$  has also disappeared, the peak at  $1641.48\text{ cm}^{-1}$  has disappeared, the peak at  $1496.78\text{ cm}^{-1}$  shifted to  $1825.1\text{ cm}^{-1}$ , the peak at  $845.66\text{ cm}^{-1}$  shifted to  $872.2\text{ cm}^{-1}$ , *Spondias mombin*, as indicated from the spectral data, results in strong adsorption.

#### Optical microscopy

Surface morphology of MS was studied by optical microscopy after 24hr immersion in 1.0 M HCl before and after addition of inhibitor. (a) represent the micrograph obtained of polished MS without being exposed to the corrosive environment while (b) showed strongly damaged MS surface due to the formation of corrosion products after immersion in 1.0 M HCl solution. Optical microscopy images of MS surface after immersion in 1.0 M HCl with 0.2g/L SM is shown in (c). It could be seen that no pits and cracks are observed in the micrographs after immersion of MS in 1.0 M HCl in the presence of inhibitors except polishing lines. Thus it revealed the presence of a good protective film upon adsorption of inhibitor molecules onto the MS surface, which was responsible for the inhibition of corrosion.





(c)

(Resolution 2048 × 1536)

Figure 12: Optical micrographs (a) polished mild steel (b) mild steel immersed in HCl and (c) HCl+ SM

**Effect of KI on the inhibition efficiency: Synergistic effect**

It is recognized that the presence of halide ions in acidic medium synergistically increases the inhibition efficiency of some organic compounds. It is assumed that the role of halide ions is to improve the adsorption of the organic cations by forming intermediate bridge between positively charged metal surface and the positive end of the inhibitor. According to Rani *et al* [10], synergism results from the increase in the surface coverage by the ion-pair interaction between organic cation and anion. Synergistic capability of the halide ion increases in order  $\text{Cl}^- < \text{Br}^- < \text{I}^-$  [8]. The greater influence of the iodide ion is considered to be due to the larger ionic radius, low electro negativity and high hydrophobicity as compared to the other halides.

**Table 9:** Weight loss data in the presence of KI with and without SM on mild steel corrosion in 1.0 M HCl and the synergism parameters

System	weight loss	%IE	$\theta$	Synergism parameter
Blank	0.065	-	-	-
0.05 M KI	0.041	36.92	0.37	-
0.2KA + 0.05 M KI	0.008	80.49	0.81	1.41
0.6KA + 0.05 M KI	0.00	90.24	0.9	1.32
1.0KA + 0.05 M KI	0.002	95.12	0.95	1.31

Inhibition efficiency of the different concentrations of SM with the 0.05 M KI is presented in Table 4. The graph plotted between inhibition efficiency and inhibitor concentration in the presence of KI is shown in figure 8. Comparison of inhibition efficiency with the KI reported in Table 4 and without KI reported in Table 1, concludes that the addition of KI shows synergistic effect with the SM

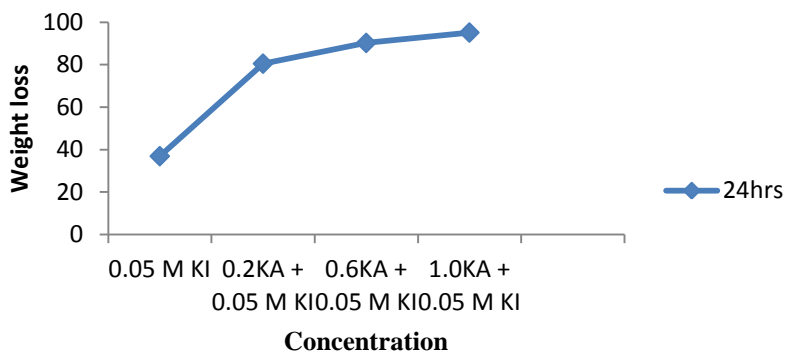


Figure 13: Plot of inhibition efficiency against various concentration of SM + 0.05M KI for mild steel corrosion in 1.0 M hydrochloric acid solution

The synergistic parameter  $S_1$ , was calculated using the relationship given by Aramaki and Hackerman:

$$S_1 = \frac{1 - i_{1+2}}{1 - i_1 + i_2} \quad (16)$$



Where,  $I_{1+2} = (I_1 + I_2)$ ,  $I_1$  = inhibition efficiency of the iodide,  $I_2$  = inhibition efficiency of *SM*,  $I_{1+2}$  = measured inhibition efficiency of *SM* in combination with iodide ion. This parameter was obtained from the inhibition efficiency values obtained from the weight loss data.  $S_1$  values calculated from eq 16 is presented in Table 4. It is clear from the data that the  $S_1$  values are greater than unity. This indicates that the improvement in the inhibition efficiency by the addition of iodide ion is due to the synergistic effect. Feng *et al.*, [17] also reported similar results. The synergistic effect of KI with *SM* is due to the stabilization of inhibitor molecule on to the mild steel surface. This stabilization may be attributed to the interaction between *SM* and  $I^-$  ions. This interaction enhances the inhibition efficiency due to the increase in the surface coverage.

## Conclusions

The corrosion inhibition potential of MS corrosion in 1.0 M HCl of *SM* was studied by weight loss, linear polarization and optical microscopy techniques. The main conclusion drawn from the studies are:

- The extracts of *SM* acted as good and efficient inhibitor for the corrosion of mild steel in HCl.
- The adsorption of the plant extracts followed Langmuir and Freundlich adsorption isotherm.
- The extracts of *SM* functioned as mixed inhibitors as obtained from the result of linear polarization.
- From the enthalpy data, the positive value of the data suggests that the reaction of the adsorption on the surface of the metal is an endothermic reaction.
- The values of entropy were positive for the extracts, indicating that the activation complex represents association steps and that the reaction was spontaneous and feasible
- The values of activation energy ( $E_a$ ) in the corrosion of mild steel in 1.0 M HCl in the presence of extract was found to be higher than that in the free acid solution which shows that the adsorbed organic matter has provided a physical barrier to change and mass transfer, leading to reduction in the rate of corrosion.
- The negative values of the free energy of adsorption indicates that the adsorption of the inhibitors on the surface of the mild steel was a spontaneous process and was found to be physisorption.
- The FTIR and Optical micrographs revealed the presence of a protective layer over the metal surface by the inhibitors through an adsorption process.

## References

1. Tao Z, Zhang S, Li W and Hou B (2009). Corrosion Science vol. 51 25-88.
2. Quraishi MA (1999). Investigation of some green compounds as corrosion and scale inhibitors for cooling systems, Corrosion, vol. 55, no. 5, Pp. 493–497.
3. Fu J, Li S, Cao L, Wang Y, Yan L (2010). Journal of Material Science. 45:979. doi:10.1007/s10853-009-4028-0ha
4. Vrsalovic L, Oguzie EE, Kliskic M, Gudic S (2011). Chemical Engineering Communications, 198, 1380–1393.
5. Njoku PC and Akumefula MI (2007). Phytochemical and nutrient evaluation of *Spondias mombin*. Pakistan Journal of Nutrition 6 (6): 613-615.
6. Ijuo G.A., Chahul H.F., Eneji I.S., (2016). Kinetic and thermodynamic studies of corrosion inhibition of mild steel using *Bridelia ferruginea* extract in acidic environment, J. Adv. Electrochem. 2(3) 107–112.
7. Oguzie EE (2008). Evaluation of the inhibitive effect of some extracts on the acid corrosion of mild steel, Corrosion Science, vol. 50. Pp.2993-2998.
8. Adeyemi OO and Olubomehin OO (2010). Investigation of *Anthoclesista djalensis* stem bark extract as corrosion inhibitor for aluminium. Pacific Journal of Science and Technology, 2010; 11:455-461.
9. Abdallah M, (2004). Antibacterial drugs as corrosion inhibitors for corrosion of aluminium in HCl solution. Corrosion Science, 46; 81-96.



10. Rani PD and Selvaraj S (2010). Inhibitive and adsorption properties of *punica granatum* extracts on brass in acid media. *Journal of phytology*, 2(11): 58-64.
11. James AO, Oforka NC, Abiola OK (2006). Inhibition of Aluminium (3SR) Corrosion in Hydrochloric acid by Pyridoxol hydrochloride. *Bulletin of Electrochemistry*, 22: 111-116.
12. Ebenso EE, Eddy NO and Odiongenyi AO (2008). Corrosion inhibitive properties and adsorption behaviour of ethanol extract of *Piper guinensis* as a green corrosion inhibitor for mildsteel in H<sub>2</sub>SO<sub>4</sub>. *Afri. J. Pure and Appl. Chem.*, 2(11): 107-115.
13. Oguzie EE, Y Li, FH Wang (2007). Corrosion inhibition and adsorption behaviour of methionine on mild steel in sulphuric acid and synergistic effect of iodide ion. *Journal of Colloid and Interface Science*, vol 310, no. 1, Pp.90-98
14. Ijuo GA, Chahul HF and Eneji IS (2016). Corrosion inhibition and adsorption behavior of *Lonchocarpus laxiflorus* extract on mild steel in hydrochloric acid. *Ew J ChemKinet* 1(1): 21-30.
15. Obot IB, Obi-Egbedi NO, Umoren SA and Ebenso EE (2010). Synergistic and antagonistic effects of anions and *Ipomoea invulcrata* as green corrosion inhibitor for aluminium dissolution in acidic medium. *Int. J. Electrochem. Science*. 5(7):994-1007.
16. Elyn Amira WAW, AA Rahim, K Awang and P Bothi Raja (2011) Evaluation of the inhibitive effect of some extracts on the acid corrosion of mild steel, *Corrosion Science* Pp 8-11.
17. Feng H Patel, SH Young, MY, (2007). Smart polymeric coatings, recent advances. *Adv. Polym. Tech.* 26:1-13

